© Indian Academy of Sciences

Long-term trend analysis of surface temperature over North-East India and adjoining regions based on CRU and ERA5 reanalysis

Rohit Gautam[1,3,*] ◉, Binita Pathak[1,2], Pradip Kumar Bhuyan[2], Arup Borgohain[3] and Shyam Sundar Kundu[3]

[1]*Department of Physics, Dibrugarh University, Dibrugarh 786 004, Assam, India.*
[2]*Centre for Atmospheric Studies, Dibrugarh University, Dibrugarh 786 004, Assam, India.*
[3]*Space and Atmospheric Science Division, North-Eastern Space Applications Centre, Umiam 793 103, Meghalaya, India.*
Corresponding author. e-mail: rohitgtm62@gmail.com

This study investigated the annual and seasonal mean temperature trends of North-East Indian region and surrounding territories over the period 1901–2020 with special emphasis on the trends from the recent past (1979–2020) utilising Climatic Research Unit (CRU) and ECMWF Reanalysis version-5 (ERA5) data. Spatio-temporal distribution of surface temperature across different seasons and associated biases between 1901 and 2020 were examined. The long-term trend of temperature was evaluated by linear regression for each month from the entire 120-yr period over the whole study domain. Further, Mann–Kendall and Sen's slope test was employed to assess the magnitude of the trend at 11 selected locations of varying altitudes. Areas around Bangladesh, which are notably polluted, as well as Myanmar and the Indian states of West Bengal, Jharkhand, Bihar and Chhattisgarh exhibited notable mean temperatures than the rest of the region. Both near-surface and 2m-temperature displayed positive trends for the period 1901–1950, 1979–2020, and during the whole duration 1901–2020, despite negative trends during 1951–1978. It has been observed that the regions with relatively higher elevations have experienced a larger warming rate than the low-elevation zones.

Keywords. Temperature; trend analysis; linear regression; Mann–Kendall and Sen's slope; CRU and ERA5; North-East India.

1. Introduction

The likelihood of significant climatic changes caused by increases in radiatively active gases in the atmosphere, a process usually referred to as 'climate change', is causing rising anxiety in both the scientific community and general public. According to the Intergovernmental Panel on Climate Change (IPCC), climate change is a shift in the state of the climate that can also be observed or identified over time (e.g., using statistical tests) – generally decades or more – by variations in the mean and/or changes in its parameters, whether brought on by natural variability or anthropogenic influences (IPCC 2007).

Global surface temperature is considered one of the crucial meteorological climate parameters that plays a vital role in altering the planetary climate system and is frequently employed to find the first indication of climate change. Other major global climate indicators, such as precipitation rate and patterns, temperature and precipitation extremes, ocean heat content, ocean acidification, concentration of atmospheric water vapour, glacier melt in continents, sea-level rise, and the frequency of intense cyclones, are all trending in the same direction as the predicted response from a warmer globe (Stocker *et al.* 2013).

In addition to the natural variability, human intervention has significantly modified the Earth's climate, particularly since the Industrial Revolution (Stocker *et al.* 2013). The activities of a quickly growing and industrialised human population have significantly increased the quantity of heat-retaining gases in the atmosphere over the past couple of centuries. The current rate of climate change, which is unparalleled in the history of modern civilisation, is one of its distinguishing features when compared to natural changes alone. Increased emissions in greenhouse gases (GHGs), aerosols, and changes in land use and land cover (LULC) throughout the industrial period were the main contributors to today's climate change, and all these factors had a considerable impact on atmospheric composition and the planetary energy balance (IPCC 2014).

The phenomenon of global warming, characterised by a substantial rise in global average surface temperatures, has emerged as one of the most critical challenges of our time, profoundly impacting both the natural biosphere and human activities (Vinnikov *et al.* 1990). Over the course of the past century, both global and local mean surface air temperatures have exhibited a significant upward trend, a well-documented phenomenon (Jones and Moberg 2003). Notably, this temperature increase has become more pronounced in recent decades, as confirmed by multiple assessments, including those from the Intergovernmental Panel on Climate Change (IPCC-AR4 2007; IPCC-AR5 2014 and references therein).

The Indian subcontinent has witnessed significant changes in climate patterns, including increased heat extremes, shifting monsoons, and rising sea levels, primarily attributed to anthropogenic climate change (Singh *et al.* 2019). Understanding the underlying mechanisms driving these changes and their potential future trajectories is of paramount importance for safeguarding lives and livelihood of people in the region. However, at the regional scale, comprehending climate change remains a formidable challenge due to the paucity of localised observational data and the intricate nature of unique physical processes (Flato *et al.* 2014). To plan for disaster management and risk mitigation, as well as develop locally applicable adaptation measures, common people and policymakers should be aware of current and predicted changes in regional climate (Burkett *et al.* 2014). It has been extensively discussed the extent to which global temperature changed in many regions during the 20th century (Cane *et al.* 1997; Reilly *et al.* 2001; Brohan *et al.* 2006; Li *et al.* 2010; Santer *et al.* 2011). The first report on the temporal fluctuations over India came in the 1950s (Pramanik and Jagannathan 1954) using observational temperature data from 30 Indian stations between 1880 and 1950. They have observed no noticeable trend in maximum and lowest temperatures. However, the average annual temperature in India was found to rise by around 0.4°C/100 years between 1901 and 1982, according to one of the early studies on modern global warming by Hingane *et al.* (1985). Srivastava *et al.* (1992) examined the decadal changes in the parameters related to climate over India between 1901 and 1986, where northern India was found to cool largely while southern India was generally warming. According to Rupa Kumar *et al.* (1994), the increasing trend in annual mean temperatures over India between 1901 and 1987 was mostly caused by an increase in maximum temperatures, while minimum temperatures remained trendless. After eliminating the global influence of greenhouse gases and natural variability, Krishnan and Ramanathan (2002) suggest that India's whole surface air temperature during the drier months of the year (January–May) has declined by as much as 0.3°C, since 1971. Kothawale and Rupa Kumar's (2005) investigation revealed that both the yearly maximum and minimum temperatures over all of India increased considerably between 1971 and 2003. Kothawale *et al.* (2010) used temperature data from the years 1901 to 2007 to conclude that there had been a considerable increase in the mean, maximum, and minimum temperatures throughout all of India and that the rate of warming has accelerated recently. Kothawale *et al.* (2012) investigated the regional and temporal asymmetry of temperature changes across India and the possible impact of aerosols.

Likewise, several studies have examined and emphasised temperature trends in India.

The present study is aimed at examining climate change and variability, particularly in temperature trends over North-East India (NEI) and surrounding territories for the past century, with special emphasis on the trends from the recent past (1979–2020), including the multidecadal variabilities till 2020.

2. Data and methodology

2.1 *Study domain and prevailing meteorology*

The study region encompasses the NEI and its adjoining regions (20°–30°N, 85°–100°E). The region has primarily four distinct seasons, viz., winter season (December–February; DJF), pre-monsoon (March–May; MAM), summer-monsoon season (June–September; JJAS), and post-mon-soon season (October–November; ON). The summers are tropical, with temperatures ranging from 23.3° to 28.3°C. Acute rainfall during the monsoon season, which spans from June to September, can bring people's lives and activity to a halt, with July experiencing the highest rainfall (565 mm). More-over, chilly Himalayan winds blowing directly into it bring the region's temperature down to 16°–18°C during winter. The mean yearly temperature of the area around the study locations is $\sim$24.4°C and mean yearly precipitations are about 2188 mm (Mitchell and Jones 2005; Harris *et al.* 2014).

To evaluate the variability in surface temperature at the local scale within the study domain and their impact on the regional climate, eleven different study locations namely, Thimphu (THM), Tawang (TWN), Shillong (SHN), Aizawl (AZL), Imphal (IPH), Banmauk (BNK), Dibrugarh (DBR), Guwa-hati (GHY), Dhubri (DHB), Agartala (AGA) and Dhaka (DAC) with varying altitudes, topography and vegetation have been selected (figure 1).

2.2 *Data source*

For temperature, data from CRU and ECMWF Reanalysis v5 (ERA5) have been utilised. CRU provided near-surface temperature at spatial resolution of 0.5° × 0.5° and 1-month temporal resolution (https://catalogue.ceda.ac.uk/uuid/c26a65020a5e4b80b20018f148556681) where units were in °C. On the other hand, the most recent high-resolution ERA5 reanalysis provided 2m-temperature (the air temperature 2 meters above the Earth's surface) data at 0.25° × 0.25° horizontal resolution (approx. 30 km) and monthly time intervals for the period 1979 to 2020 (https://cds.climate.copernicus.eu), where units were converted from Kelvin to °C.

2.2.1 *CRU*

The Climatic Research Unit data (v4.05) of near-surface temperature at 0.5° ($\sim$55 km) spatial res-olution on monthly temporal resolution during 1901–2020 was utilised in this study. These data-sets are available over only land areas of the world (except Antarctica) and can be accessed online at https://crudata.uea.ac.uk. Harris *et al.* (2020) may be consulted for further information on the proce-dure involved in obtaining these monthly climate observational datasets.

An interpolation technique called angular-distance weighting (ADW) was used to develop the CRU Time-Series (TS) 4.05 data. IDL triangula-tion routines were utilised in all versions until 4.00.

2.2.2 *ERA5*

Data from the fifth generation of atmospheric reanalysis of the global climate (ERA5) from the European Centre for Medium-Range Weather Fore-casts (ECMWF) and produced by Copernicus Cli-mate Change Service (C3S) was also utilised. From 1979 to the present, ERA5 climatic data cover the entire land and ocean domain of the world and are accessible in a 0.25°×0.25° grid (Hersbach *et al.* 2018). For the duration of 1979–2020, the monthly temperature data was accessed from https://cds.climate.copernicus.eu/cdsapp#!/dataset/reanalysis-era5-single-levels-monthly-means?tab=form.

The ERA5 datasets are the most recent version of the ECMWF's 5-day real-time global atmo-spheric reanalysis from 1979 (Hersbach and Dee 2016) and replaces the ERA-Interim reanalysis (Dee *et al.* 2011). The ECMWF provides estimates for a wide variety of atmospheric, land-based, and oceanic weather and climate variables every hour and every six hours. The data resolve the atmo-sphere using 137 levels from the Earth's surface up to an altitude of 80 km, covering the planet on a grid of approximately 30 km. ERA5 incor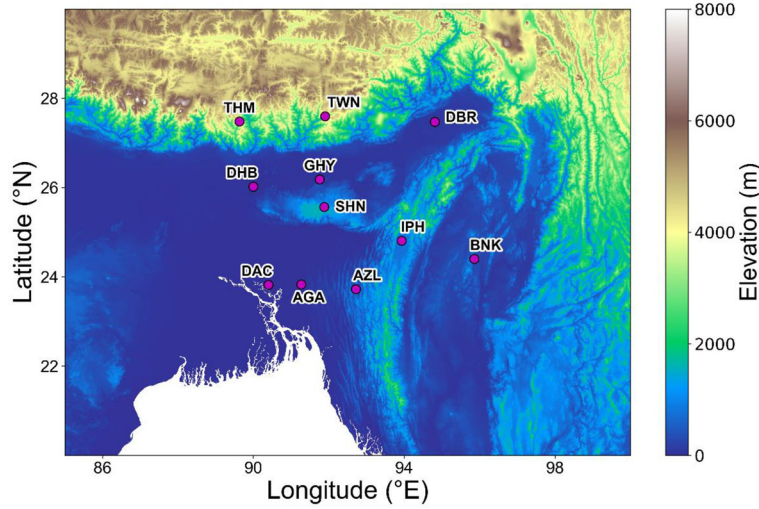porates data at decreased spatial and temporal resolutions (https://www.ecmwf.int/en/forecasts/datasets/reanalysis-datasets/era5).

Figure 1. A topographic view of the study domain showing 11 different locations used in the study.

2.3 Methodology

2.3.1 Mann–Kendall trend analysis

Since a non-parametric test may avoid the issue caused by data skew, it is preferable over a parametric test (Smith 2000). When several stations are assessed in a single study, the Mann–Kendall (MK) test is usually favoured (Hirsch *et al.* 1991).

The MK test is a distribution-free test for estimating a time series trend (Mann 1945; Kendall 1975), i.e., even if the time series do not adhere to a certain distribution, it may be employed. The test assumes that the data are not serially correlated and largely depends on the quantity of data points. The first point is true for all statistical tests; however, the second cannot be done if comparing data sets from several time periods is the goal. We deal with a lot of data like this in trend analysis. A non-parametric regression approach called Sen's slope (SS) test is almost always used in conjunction with the MK test to evaluate the trend magnitude and to know whether the y values are going up or down over time.

The MK test statistics (S) is expressed as (Salas 1993) follows:

$$S = \sum_{i=1}^{n-1} \sum_{j=i+1}^{n} \mathrm{sgn}(x_j - x_i).$$

Here, n denotes the number of records, x_i and x_j are the data values for the time series i and j (where $j > i$), respectively and $\mathrm{sgn}(x_j - x_i)$ is the sign function defined as:

$$\mathrm{sgn}(x_j - x_i) = \begin{cases} 1, & \text{if } (x_j - x_i) > 0 \\ 0, & \text{if } (x_j - x_i) = 0 \\ -1, & \text{if } (x_j - x_i) < 0 \end{cases}.$$

For all the differences considered, this statistic represents the number of negative differences. The test is carried out using a normal distribution (Helsel and Hirsch 1992) with the mean and variance as follows, for large samples ($n > 10$).

$$E[S] = 0$$

$$\mathrm{Var}(S) = \frac{n(n-1)(2n+5) - \sum_{i=1}^{m} t_i(t_i - 1)(2t_i + 5)}{18}$$

where n indicates the overall number of data points; t_i, the number of ties of size i; and m, the number of coupled groups. Here, coupled groups refer to a collection of data points of the same kind. The standard normal test statistic Z_s (Z-statistics) is calculated when there are more than 10 data points ($n > 10$) using (Hirsch *et al.* 1993):

$$Z_s = \begin{cases} \dfrac{S-1}{\sqrt{\mathrm{Var}(S)}}, & \text{when } S > 0 \\ 0, & \text{when } S = 0 \\ \dfrac{S+1}{\sqrt{\mathrm{Var}(S)}}, & \text{when } S < 0 \end{cases}.$$

An upward trend is shown when Z_S is more than zero, while a downward trend is indicated when Z_S is less than zero. The alternative hypothesis (H_1) is

chosen if there is a positive or negative trend in the variable, whereas the null hypothesis (H_0) is chosen if there is no trend. If $|Z_S| > Z_{1-\alpha/2}$, a strong trend is detected in the data series, and the null hypothesis is discarded. The normal distribution table in its conventional form may be used to determine the value of $Z_{1-\alpha/2}$. If $|Z_S| > 1.96$ at the 5% significance level ($\alpha = 0.05$) as determined by the standard normal cumulative distribution chart, the null hypothesis of no trend is rejected (Lund *et al.* 2007; Costa and Soares 2009). The significance levels, $\alpha = 0.01\,(99\%), 0.05\,(95\%)$ and $0.1\,(90\%)$, were employed in this investigation.

Sen's slope estimator (Sen 1968), a nonparametric technique, is applied in the study of climatic time series and is employed by many researchers (Lettenmaier *et al.* 1994; Yunling and Yiping 2005; Partal and Kahya 2006; El-Nesr *et al.* 2010; Tabari *et al.* 2011, 2012). Sen's method, which is frequently employed to assess the strength of trends in hydrometeorological time series, presupposes a linear trend in the time series (Lettenmaier *et al.* 1994; Yue and Hashino 2003; Partal and Kahya 2006). It roughly represents the trend slope, Q, in the sample of N pairs of data points and is calculated as the median of:

$$Q_i = \frac{x_j - x_k}{j - k}, \quad i = 1, 2, \ldots, N.$$

where x_j and x_k are the data values at times j and k ($k > j$), respectively, i.e., Sen's slope, $Q = $ median (Q_i).

2.3.2 *Linear regression*

A statistical technique called simple linear regression analysis is used to establish or investigate the relationship between two variables of interest. In this regression model, one variable is called an explanatory (independent) variable, and the other one is a response (dependent) variable. The regression coefficients β_0 and β_1 in the following equation are estimated through linear regression:

$$y = \beta_0 + \beta_1 x + \varepsilon$$

where y is the study variable (or dependent variable) and x is the explanatory variable (or independent variable). β_0 and β_1 are termed as an intercept term (a constant) and the slope parameter/coefficient for the variable x, respectively. The component, ε, also known as the residuals, is the unobservable error component or the model's error term. It is responsible for the data's inability to fall

in a straight line and reflects the mismatch between the true and observed realisations of y. It is important to note that the aforementioned equation yields y from x. The residual includes the effects of all the various causes on the value of y.

3. Results and discussion

Distinct variability in temperature trends both at spatial and temporal scales during the period 1901–2020 over NEI and surrounding areas was observed (figure 2). The spatial distribution of near-surface temperature during four seasons (MAM, JJA, SON, DJF) retrieved from CRU for 1901 and 2020, as well as associated biases are shown in figure 2. Since the available data series from CRU was relatively lengthy (about 120 years), it was divided into three sub-periods: (a) pre-satellite era (1901–1950), (b) transition era (1951–1978), and (c) satellite era (1979–2020), to perform the trend analysis. By examining the era of pre-satellite, which represents the early 20th century, a time before the availability of satellite-based observations, we aimed to capture the trends and patterns in climate that predate modern observational tools, allowing us to establish a baseline for natural climate variability. The mid-20th century marks the advent of satellite technology, providing a more comprehensive and global perspective on climate phenomena, and the inclusion of this period allows us to assess the impact of improved observational capabilities on our understanding of climate dynamics and to identify any noticeable transitions or changes in trends. The last period encompassing the era of advanced satellite observations marks the deployment of satellites that have significantly enhanced our ability to monitor various climate variables with higher spatial and temporal resolution. This phase is crucial for examining recent trends, identifying anomalies, and assessing the influence of human activities on observed climate changes. By partitioning the analysis into these three blocks, we aimed to delineate the coaction of natural and anthropogenic factors over distinct periods in the history of climate research, which in turn allows us to discern better long-term trends, potential abrupt shifts, and the impact of technological advancements on our understanding of climate variability. Mann–Kendall and Sen's slope test statistics results for monthly mean near-surface temperature during 1901–1950, 1951–1978 and 1979–2020 based on CRU, and 2m-temperature during 1979–2020 based on ERA5, for the study region, are presented in table 1.
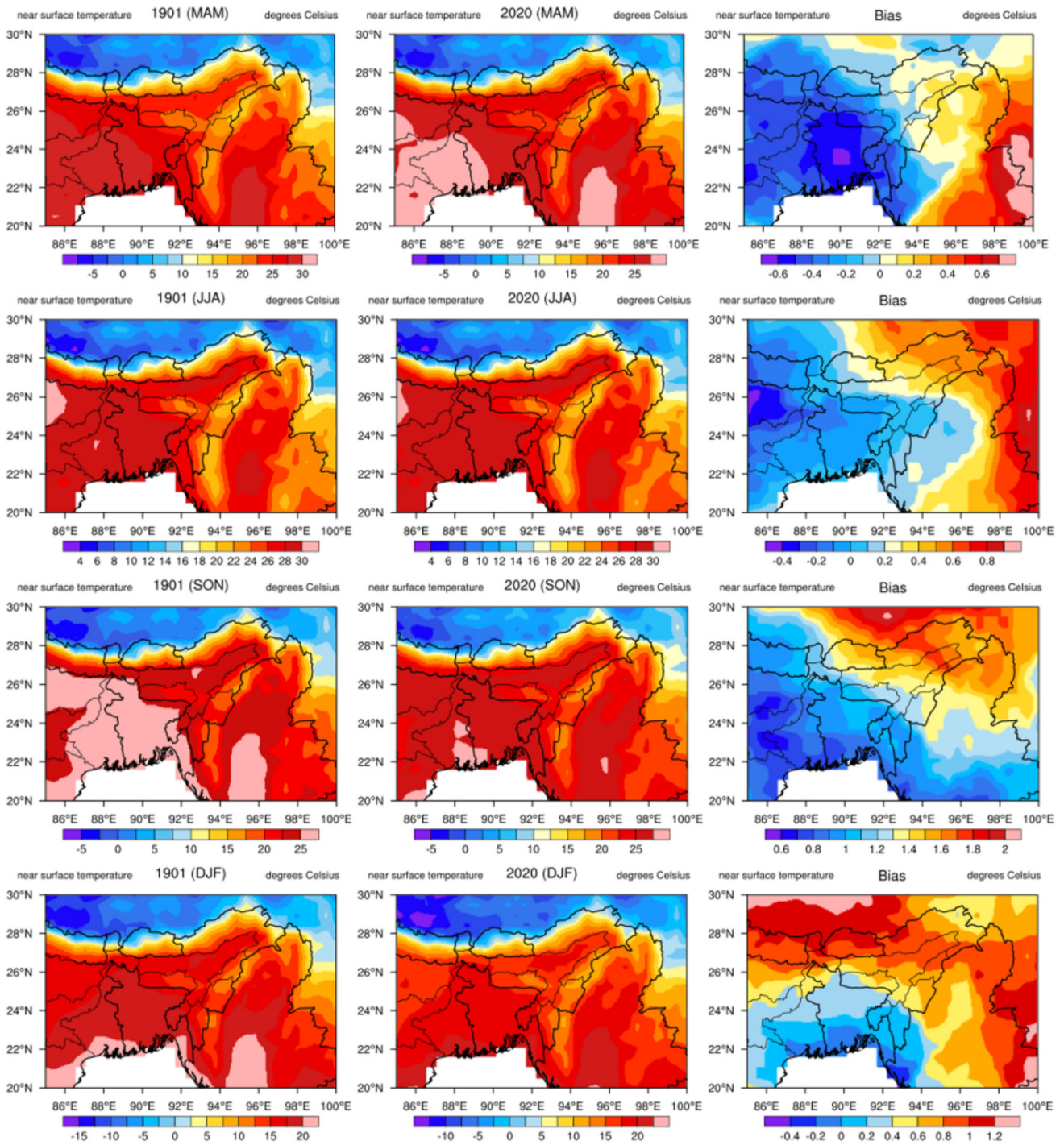
Figure 2. Spatial distribution of near-surface temperature in 1901, 2020 and bias for the seasons: **(a)** pre-monsoon (MAM), **(b)** summer/monsoon (JJA), **(c)** post-monsoon (SON), and **(d)** winter (DJF), based on CRU.

3.1 *Spatiotemporal distribution of near-surface temperature*

For each year in consideration, near-surface mean temperatures to the north of ∼28°N were relatively on the lower side, whereas to the south of ∼28°N, the temperatures were generally higher (figure 2). Areas around Bangladesh, which are notably polluted, as well as parts of Myanmar and the Indian states of West Bengal, Bihar, Jharkhand and Chhattisgarh exhibited greater mean temperatures than the rest of the region, in general. The post-monsoon season (SON) displayed a temperature rise (∼0.6°–2°C) over the entire region with gradually increasing magnitudes from the southwestern region to the northeastern stretches

Table 1. *Results of Mann–Kendall and Sen's slope test for near-surface temperature from CRU and 2-m temperature from ERA5 averaged over the entire NEI and adjoining regions at different time periods.*

Month		CRU (1901–1950)	CRU (1951–1978)	CRU (1979–2020)	ERA5 (1979–2020)
JAN	Z	2.08**	–0.26	1.41	1.3
	Q	0.01	0	0.02	0.01
FEB	Z	2.24**	–0.73	2.1**	2.34**
	Q	0.01	–0.02	0.02	0.03
MAR	Z	2.12**	0.57	1.5	1.42
	Q	0.02	0.01	0.01	0.01
APR	Z	1.79*	–1.98**	0.5	0.59*
	Q	0.01	–0.03	0.01	0.01
MAY	Z	1.84*	–1.96*	1.83*	1.27
	Q	0.01	–0.02	0.01	0.01
JUN	Z	1.25	–1.32	1.77*	2.88***
	Q	0.01	–0.01	0.01	0.02
JUL	Z	1.35	–0.26	2.81***	4.15***
	Q	0.01	0	0.01	0.02
AUG	Z	3.66***	–1.01	2.69***	4.89***
	Q	0.01	–0.01	0.01	0.02
SEP	Z	2.63***	–0.61	3.12***	4.95***
	Q	0.01	–0.01	0.02	0.03
OCT	Z	1.41	–0.14	1.76*	2.97***
	Q	0.01	0	0.01	0.03
NOV	Z	2.43**	0.45	2.34**	2.86***
	Q	0.01	0.01	0.02	0.03
DEC	Z	4.12***	–1.64	1.99**	2.1**
	Q	0.03	–0.02	0.02	0.02

***, **, and * indicate that the trends are significant at 99%, 95% and 90% level of confidence, respectively. Minus sign indicates that the trend is decreasing.

of the study domain between 1901 and 2020. However, the winter season (DJF) showed a rise in temperatures for most parts of the area except a tiny portion near southern Bangladesh, West Bengal and eastern Myanmar, where an insignificant fall in temperatures ($\sim$0.4°–0.1°C) was observed. During the monsoon season (JJA), although the areas experiencing a fall in temperatures were relatively greater, there was a rise in temperatures observed for most parts of the areas lying east of the study domain ($\sim$0.2°–0.9°C). The pre-monsoon season (MAM) showed a similar tendency, with the southeastern regions seeing the largest rise in mean temperatures ($\sim$0.4°–0.8°C) during the same time period.

3.2 *Trend analysis of surface temperature*

During the last 120-year period, there has been an increasing trend of magnitude $\sim$0.11°C decade^{-1} in February, followed by $\sim$0.10°C decade^{-1} in December and up to $\sim$0.02°C decade^{-1} in July

(figure 3). The trend analyses for other sub-periods were performed using M–K and Sen's slope test (table 1).

The time series of surface temperature across various months revealed significant warming trends for the mean annual temperatures during the most recent period, 1979–2020, as compared to the variability in the past century (1901–2020) and periods like 1901–1950, 1951–1978 over the entire NEI and adjoining areas. However, the duration 1951–1978 exhibited declining trends for most of the months.

During the first half of the previous century (1901–1950), all the months exhibited increasing trends, with a maximum increase in December ($\sim$0.3°C decade^{-1}) followed by March ($\sim$0.2°C decade^{-1}) at 99% and 95% confidence level, respectively (table 1). The temperature increases at a rate of $\sim$0.1°C decade^{-1} in the rest of the months, at a 99% significance level in August and September; at 95% level in January, February and November; at 90% level in April and
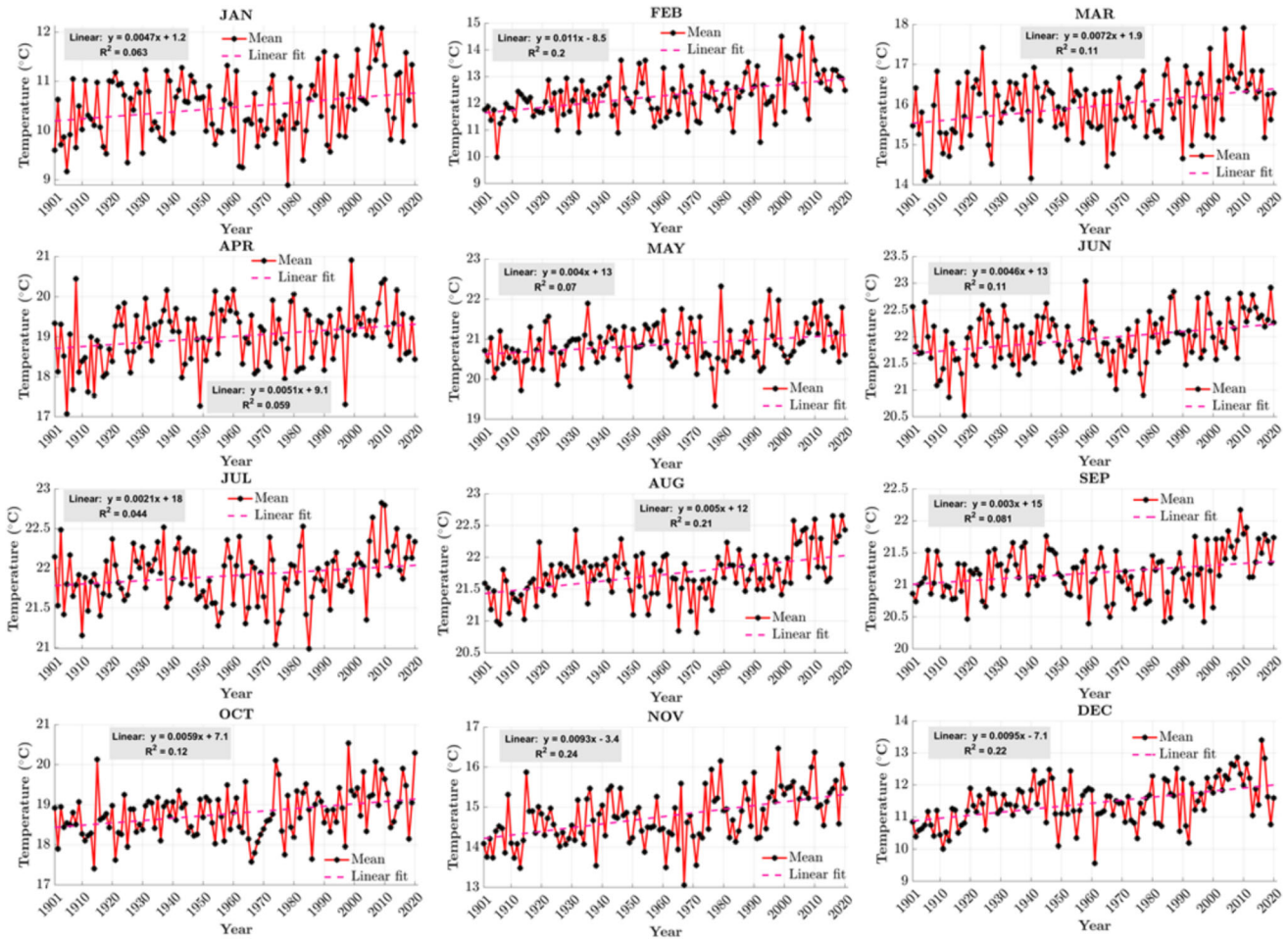
Figure 3. Temporal variation of near-surface temperature across various months, retrieved from CRU, over the NEI and adjoining land areas for the period of 1901–2020. The dashed line through the data points represents the linear least square fit indicating the long-term trend in 2m-temperature, its slope yielding the trend (°C/yr).

May and a non-significant increase in June, July and October. Between 1951 and 1978, the majority of the months displayed declining temperature trends, although non-significant, with the exception of March and November. However, in April and May, the decrease is significant with a rate of ~ 0.3°C decade^{-1} at 95% level of significance and ~ 0.2°C decade^{-1} at 90% level, respectively. Contrarily, a relatively higher warming rate was observed in the most recent period (1979–2020), especially during the months of summer monsoon (JJAS), post-monsoon (ON) and winter (DJF) seasons for both CRU and ERA5. Warming at a rate of ~ 0.1°C decade$^{-1}/\sim 0.2$°C decade^{-1} to ~ 0.2°C decade$^{-1}/\sim 0.3$°C decade^{-1} at 99% confidence interval was observed in July, August and September for both the data sources. Similarly, warming in the winter months of December and February at a rate of ~ 0.2°C decade^{-1} and ~ 0.2°C decade$^{-1}/\sim 0.3$°C decade^{-1} at a 95% confidence interval was observed. For CRU, May,

June and October exhibited a warming of ~ 0.1°C decade^{-1} at 90% significance level, while for ERA5, it was observed only during April. However, in November, the former shows a warming of ~ 0.2°C decade^{-1} at the 95% level and the latter exhibited the same at ~ 0.3°C decade^{-1} at the 99% level. The warming was observed to be non-significant during January and March for both type of data sets. It is worth mentioning here that the spatial resolution for ERA5 ($0.25° \times 0.25°$) is finer than that of CRU ($0.5° \times 0.5°$).

Mann–Kendall and Sen's slope test revealed an overall significant warming trend for each of the 11 locations over the decades with large variability in magnitude ranging between 0.1° and 0.5°C decade^{-1} mostly at 99% significance level during June–November (table 2). However, the warming in November at SHN, DHB, and DAC and that in October at THM and TWN were at 95% level, while at AGA, the same was at 90%. Moreover, a non-significant warming trend was observed over

Table 2. *Results of Mann–Kendall and Sen's slope test for 2m-temperature trend at different locations for the period 1979–2020 using ERA5.*

Month		THM	TWN	SHN	AZL	IPH	BNK	DBR	GHY	DHB	AGA	DAC
JAN	Z	1.28	1.56	1.63	1.46	2.73***	1.5	2.06**	1.04	-0.85	-1.13	-2.15**
	Q	0.02	0.04	0.02	0.01	0.03	0.01	0.02	0.01	-0.01	-0.01	-0.02
FEB	Z	2.64***	2.60***	3.12***	3.17***	3.92***	2.43**	2.89***	2.34**	1.1	1.95*	1.28
	Q	0.05	0.05	0.04	0.04	0.05	0.04	0.04	0.03	0.02	0.02	0.02
MAR	Z	2.26**	1.80*	2.76***	2.85***	3.73***	1.34	2.28**	1.70*	0.33	1.59	1.19
	Q	0.03	0.03	0.03	0.04	0.04	0.02	0.03	0.02	0	0.02	0.01
APR	Z	1.06	1.74*	1.67*	1.95*	1.59	0.29	2.22**	0.31	-0.9	1.21	0.72
	Q	0.01	0.02	0.02	0.03	0.03	0.01	0.02	0	-0.01	0.02	0.01
MAY	Z	1.21	2.24**	2.42**	2.47**	2.05**	-0.31	0.25	1.05	0.97	2.16**	1.95*
	Q	0.01	0.02	0.02	0.03	0.02	-0.01	0	0.01	0.01	0.03	0.02
JUN	Z	3.91***	3.52***	2.85***	3.69***	3.51***	3.77***	0.31	1.15	1.9**	2.74***	2.85***
	Q	0.02	0.02	0.01	0.02	0.02	0.04	0	0.01	0.02	0.02	0.02
JUL	Z	4.86***	4.57***	5.12***	4.86***	4.90***	3.87***	3.68***	4.37***	4.28***	4.56***	4.6***
	Q	0.03	0.03	0.03	0.03	0.03	0.03	0.03	0.03	0.03	0.03	0.03
AUG	Z	5.07***	4.90***	4.64***	4.78***	5.15***	5.38***	2.33**	3.47***	4.05***	4.76***	5.23***
	Q	0.03	0.03	0.03	0.03	0.03	0.04	0.02	0.03	0.03	0.03	0.03
SEP	Z	4.83***	4.70***	5.57***	5.98***	5.53***	5.30***	4.38***	4.94***	4.88***	5.81***	5.03***
	Q	0.03	0.03	0.03	0.04	0.04	0.05	0.04	0.03	0.03	0.03	0.03
OCT	Z	2.08**	2.14**	4.01***	4.33***	4.05***	3.83***	4.00***	4.36***	4.32***	4.01***	2.99***
	Q	0.03	0.03	0.03	0.03	0.04	0.03	0.04	0.03	0.03	0.03	0.02
NOV	Z	2.77***	2.80***	2.38**	2.59***	2.92***	3.19***	1.19	2.72***	2.24**	1.66*	2.02**
	Q	0.05	0.04	0.03	0.03	0.03	0.03	0.01	0.03	0.02	0.02	0.01
DEC	Z	3.06***	2.80***	1.59	1.86*	2.53**	2.32**	1.34	1.56	0.35	0.54	-0.3
	Q	0.07	0.05	0.02	0.02	0.02	0.03	0.01	0.02	0	0	0

***, **, * indicate that the trends are significant at 99%, 95% and 90% level of confidence, respectively. Minus sign indicates that the trend is decreasing.
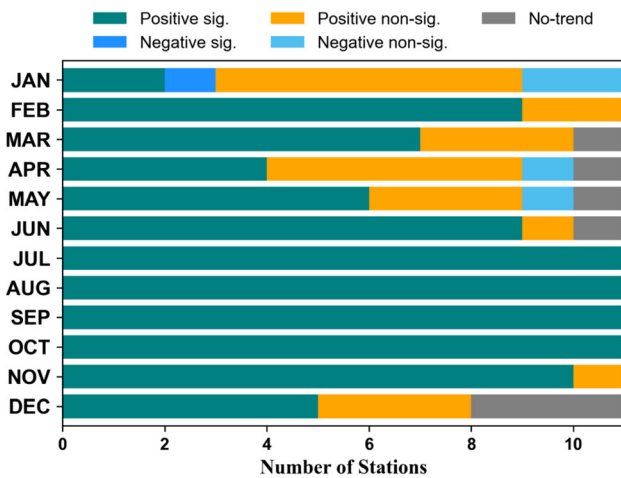
Figure 4. Number of stations showing positive (increasing) significant and non-significant; negative (decreasing) significant and non-significant at 90% level of significance; and no-trend across different months during 1979–2020, based on ERA5.

DBR. In December, however, high latitude locations such as TWN and THM exhibited the highest warming rate of 0.5°C decade^{-1} and 0.7°C decade^{-1}, respectively, at 99% confidence level, followed by BNK and IPH, where warming was at a rate of 0.3°C decade^{-1} and 0.2°C decade^{-1}, respectively at 95% confidence level. The rate for the month of December in AZL was 0.2°C decade^{-1} at a 90% level, while the same in the low-altitude locations were non-significant. However, in DAC, temperature trends decreased non-significantly during December and at a confidence interval of 95% during January. The locations close to DAC, viz. DHB and AGA also exhibited non-significant decreasing temperature trends in January. Strong warming trends prevailed in February over most of the locations, with steeper increasing trends with increasing altitudes, the maximum rate being over THM, TWN and IPH (0.5°C decade^{-1}) at a 99% confidence level. March, April and May also showed significant trends across stations with greater elevations ranging between 0.2 and 0.4°C decade^{-1} and relatively higher trend magnitudes at AZL and IPH. The months of February and between June and November were found to be the time with the greatest number of stations exhibiting significant increasing trends (figure 4).

4. Summary and conclusions

The broad spatiotemporal variability in temperature over NEI and the neighbouring areas is caused by the non-uniform distribution of GHGs, aerosols,

and particulate matter in the area (Gogoi *et al.* 2009; Pathak *et al.* 2016; Biswas *et al.* 2017; Pathak and Bhuyan 2022). Pollution attributable to human activity due to a relatively larger population is the primary cause of areas around Bangladesh, Myanmar and the Indian states of West Bengal, Jharkhand, Chhattisgarh and Bihar displaying greater mean temperatures than the rest of the region (Sharma 2003). While both the pre-satellite and satellite eras displayed only a rise in mean annual temperature, the transition era showed both increases and decreases in temperature across different months. Nevertheless, the last four decades showed a tendency towards a warmer climate over the region mainly due to increased anthropogenic activities. Both near-surface and 2m-temperature displayed positive trends for the period 1901–1950, 1979–2020 and during the whole duration 1901–2020.

With changes in height and orographic winds further altering the temperature gradient along various elevation belts, the temperature across the study region is very unpredictable. Additionally, seasonal variations in solar insolation and the amount of available atmospheric moisture influence it. Temperature fields with sharp variations show the region's vulnerability to climate change. It has been observed that regions with higher elevation have experienced a higher warming rate than regions with low elevation. The warming rate is found to be maximum during JJAS at $\sim$1000–3000 m elevation belt, which includes locations such as THM, TWN, SHN and AZL. The NEI's TWN area has the highest warming rate of 0.5°C decade^{-1}. Except for January, all of the summer (JJAS), post-monsoon (ON), and winter (DJF) months showed a larger warming rate for most of the sites, indicating a longer summer and warmer winter and, thus a changing general climate prevailing over the region.

Over the area, the surface temperature is generally on the rise. Trends are driven by trace gases, especially GHGs and aerosols, including PM, emitted primarily by anthropogenic activities due to the growing population accompanied by increasing urbanisation, changes in land use, major roadway expansions, increased deforestation, biomass burning, fossil fuel consumption, leading to an increasing concentration of gaseous constituents including greenhouse gases (GHGs) and aerosols (Mitchell *et al.* 1995). Despite being less inhabited and having less industrial and human activities than the rest of India, the region serves as a sink to

the emissions from the industrialised west and highly populated Indo-Gangetic plains (IGP), where the concentration of both gaseous pollutants and particulate matter is relatively high. The climate prevailing over the NEI and the surrounding regions is conducive for not only formation but also redistribution and thus accumulation of both local and remote atmospheric composition particularly in dry months (Pathak and Bhuyan 2022).

Due to climate change, crop production in the region can be affected. Extreme weather due to a change in the climate might occasionally cause crop damage, whereas long-term changes in means or climate variability can have an impact on agricultural production. Modelling of the impact of increasing temperature means and variability on agricultural output has shown that crop productivity decreases when temperature variability rises in various situations (Semenov and Porter 1995; Mearns *et al.* 1996; Riha *et al.* 1996).

Seasonal temperature variations in the region, in particular, surface temperature trends, can significantly influence the monsoon's activity and the effects it has on agricultural production. With summers extending beyond September and winters getting shorter and warmer, this indicates a significant acceleration of the warming over the past four decades, the effect being majorly felt in relatively higher altitude areas and is consistent with current global trends. According to the results of the current study, the future climate of the NEI will experience warming/wetter scenarios as a result of a rise in temperature. The biodiversity, hydrology, and ecosystems in the area may be dramatically affected further by this forecasted scenario.

Acknowledgements

Author statement

Rohit Gautam was responsible for investigation, data curation, software, methodology, visualisation, formal analysis and writing original draft of the manuscript. Binita Pathak and P K Bhuyan were responsible for conceptualisation, supervision, validation, analysis and reviewing of the manuscript. Arup Borgohain and S S Kundu were responsible for overall supervision and reviewing of the manuscript.

References

Biswas J, Pathak B, Patadia F, Bhuyan P K, Gogoi M M and Babu S S 2017 Satellite-retrieved direct radiative forcing of aerosols over North-East India and adjoining areas: Climatology and impact assessment; *Int. J. Climatol.* **37(S1)** 298–317, https://doi.org/10.1002/joc.5325.

Brohan P, Kennedy J J, Harris I, Tett S F and Jones P D 2006 Uncertainty estimates in regional and global observed temperature changes: A new data set from 1850; *J. Geophys. Res. Atmos.* **111(D12)**, https://doi.org/10.1029/2005JD006548.

Burkett V R, Suarez A G, Bindi M, Conde C, Mukerji R, Prather M J, St Clair A L anf Yohe G W 2014 Point of departure; In: *Climate change 2014: Impacts, adaptation, and vulnerability. Part A: global and sectoral aspects* (eds) Field C B, Barros V R, Dokken D J, Mach K J, Mastrandrea M D, Bilir T E, Chatterjee M, Ebi K L, Estrada Y O, Genova R C, Girma B, Kissel E S, Levy A N, MacCracken S, Mastrandrea P R and White L L, Contribution of Working Group II to the fifth assessment report of the Intergovernmental Panel on Climate Change; Cambridge University Press, pp. 169–194.

Cane M A, Clement A C, Kaplan A, Kushnir Y, Pozdnyakov D, Seager R, Zebiak S E and Murtugudde R 1997 Twentieth-century sea surface temperature trends; *Sci.* **275(5302)** 957–960, https://doi.org/10.1126/science.275.5302.957.

Costa A C and Soares A 2009 Homogenization of climate data: Review and new perspectives using geostatistics; *Math. Geosci.* **41(3)** 291–305, https://doi.org/10.1007/s11004-008-9203-3.

Dee D P, Uppala S M, Simmons A J, Berrisford P, Poli P, Kobayashi S and Vitart F 2011 The ERA-Interim reanalysis: Configuration and performance of the data assimilation system; *Quart. J. Roy. Meteorol. Soc.* **137(656)** 553–597, https://doi.org/10.1002/qj.828.

El-Nesr M N, Abu-Zreig M M and Alazba A A 2010 Temperature trends and distribution in the Arabian Peninsula; *Am. J. Environ. Sci.* **6(2)** 191–203, https://doi.org/10.3844/ajessp.2010.191.203.

Flato G, Marotzke J, Abiodun B, Braconnot P, Chou S C, Collins W, Cox P, Driouech F, Emori S, Eyring V and Forest C 2014 Evaluation of climate models; In: *Climate change 2013: The physical science basis*, Contribution of Working Group I to the Fifth Assessment Report of the Intergovernmental Panel on Climate Change; Cambridge University Press, pp. 741–866.

Gogoi M M, Krishna Moorthy K, Babu S S and Bhuyan P K 2009 Climatology of columnar aerosol properties and the influence of synoptic conditions: First-time results from the northeastern region of India; *J. Geophys. Res. Atmos.* **114(D8)**, https://doi.org/10.1029/2008JD010765.

Harris I P D J, Jones P D, Osborn T J and Lister D H 2014 Updated high-resolution grids of monthly climatic observations – the CRU TS3 10 Dataset; *Int. J. Climatol.* **34(3)** 623–642, https://doi.org/10.1002/joc.3711.

Harris I, Osborn T J, Jones P and Lister D 2020 Version 4 of the CRU TS monthly high-resolution gridded multivariate climate dataset; *Scientific Data* **7(1)**, https://www.nature.com/articles/s41597-020-0453-3.

Hersbach H, Rosnay P De, Bell B, Schepers D, Simmons A, Soci C, Abdalla S, Alonso-Balmaseda M, Balsamo G, Bechtold P and Berrisford P 2018 Operational global reanalysis: Progress future directions and synergies with NWP; *ERA Report Series no. 27, ECMWF: Reading, UK*, https://doi.org/10.21957/tkic6g3wm.

Hersbach H and Dee D 2016 ERA5 reanalysis is in production; *ECMWF Newsletter* **147(7)** 5, https://www.ecmwf.int/en/newsletter/147/news/era5-reanalysis-production.

Helsel D R and Hirsch R M 1992 Statistical methods in water resources; *Techniques and Methods 4-A3*, Elsevier Science, New York, https://doi.org/10.3133/tm4A3.

Hingane L S, Rupa Kumar K and Ramana Murty B V 1985 Long-term trends of surface air temperature in India; *Int. J. Climatol.* **5(5)** 521–528, https://doi.org/10.1002/joc.3370050505.

Hirsch R M, Helsel D R, Cohn T A and Gilroy E J 1993 Statistical treatment of hydrologic data; In Handbook of hydrology (ed.) Maidment D R, McGraw-Hill: New York, pp. 17.1–17.52.

Hirsch R M, Alexander R B and Smith R A 1991 Selection of methods for the detection and estimation of trends in water quality; *Water Resour. Res.* **27(5)** 803–813, https://doi.org/10.1029/91WR00259.

IPCC-AR4 2007 *Climate Change 2007, The Scientific Basis*; Contribution of Working Group I to the Fourth Assessment Report of Intergovernmental Panel on Climate Change (IPCC), Cambridge University Press, Cambridge.

IPCC-AR5 2014 *Climate Change 2014, The Scientific Basis*; Contribution of Working Group I to the Fourth Assessment Report of Intergovernmental Panel on Climate Change (IPCC), Cambridge University Press, Cambridge.

Jones P D and Moberg A 2003 Hemispheric and large-scale surface air temperature variations: An extensive revision and an update to 2001; *J. Clim.* **16(2)** 206–223, https://doi.org/10.1175/1520-0442(2003)016%3C0206:HALSSA%3E2.0.CO;2.

Kendall M G 1975 *Rank correlation methods*; 4th edn. Charles Griffin, London, UK.

Kothawale D R, Kumar K K and Srinivasan G 2012 Spatial asymmetry of temperature trends over India and possible role of aerosols; *Theor. Appl. Climatol.* **110(1)** 263–280, https://doi.org/10.1007/s00704-012-0628-8.

Kothawale D R, Munot A A and Kumar K K 2010 Surface air temperature variability over India during 1901–2007, and its association with ENSO; *Clim. Res.* **42(2)** 89–104, https://doi.org/10.3354/cr00857.

Kothawale D R and Rupa Kumar K 2005 On the recent changes in surface temperature trends over India; *Geophys. Res. Lett.* **32(18)**, https://doi.org/10.1029/2005GL023528.

Krishnan R and Ramanathan V 2002 Evidence of surface cooling from absorbing aerosols; *Geophys. Res. Lett.* **29(9)** 54-1–54-4, https://doi.org/10.1029/2002GL014687.

Lettenmaier D P, Wood E F and Wallis J R 1994 Hydro-climatological trends in the continental United States, 1948–1988; *J. Clim.* **7(4)** 586–607, https://doi.org/10.1175/1520-0442(1994)007%3c0586:HCTITC%3e2.0.CO;2.

Li Q, Dong W, Li W, Gao X, Jones P, Kennedy J and Parker D 2010 Assessment of the uncertainties in temperature change in China during the last century; *Chin. Sci. Bull.* **55** 1974–1982, https://doi.org/10.1007/s11434-010-3209-1.

Lund R, Wang X L, Lu Q Q, Reeves J, Gallagher C and Feng Y 2007 Changepoint detection in periodic and autocorrelated time series; *J. Clim.* **20(20)** 5178–5190, https://doi.org/10.1175/JCLI4291.1.

Mann H B 1945 Nonparametric tests against trend; *Econometrica: J. Econom. Soc.* **13** 245–259, https://doi.org/10.2307/1907187.

Mearns L O, Rosenzweig C and Goldberg R 1996 The effect of changes in daily and interannual climatic variability on CERES-wheat: A sensitivity study; *Clim. Chang.* **32(3)** 257–292, https://doi.org/10.1007/BF00142465.

Mitchell T D and Jones P D 2005 An improved method of constructing a database of monthly climate observations and associated high-resolution grids; *Int. J. Climatol.* **25(6)** 693–712, https://doi.org/10.1002/joc.1181.

Mitchell J F, Johns T C, Gregory J M and Tett S F B 1995 Climate response to increasing levels of greenhouse gases and sulphate aerosols; *Nature* **376(6540)** 501–504, https://doi.org/10.1038/376501a0.

Partal T and Kahya E 2006 Trend analysis in Turkish precipitation data; *Hydrol. Process.* **20(9)** 2011–2026, https://doi.org/10.1002/hyp.5993.

Pathak B and Bhuyan P K 2022 Characteristics of atmospheric pollutants over the northeastern region of India; In: *Asian atmospheric pollution,* Elsevier, pp. 367–392, https://doi.org/10.1016/B978-0-12-816693-2.00016-0.

Pathak B, Subba T, Dahutia P, Bhuyan P K, Moorthy K K, Gogoi M M and Singh S B 2016 Aerosol characteristics in north-east India using ARFINET spectral optical depth measurements; *Atmos. Environ.* **125** 461–473, https://doi.org/10.1016/j.atmosenv.2015.07.038.

Pramanik S K and Jagannathan P 1954 Climatic changes in India – (II) Temperature; *Mausam* **5(1)** 29–47, https://doi.org/10.54302/mausam.v5i1.4845.

Reilly J, Stone P H, Forest C E, Webster M D, Jacoby H D and Prinn R G 2001 Uncertainty and climate change assessments; *Sci.* **293(5529)** 430–433, https://doi.org/10.1126/science.1062001.

Riha S J, Wilks D S and Simoens P 1996 Impact of temperature and precipitation variability on crop model predictions; *Clim. Chang.* **32(3)** 293–311, https://doi.org/10.1007/BF00142466.

Rupa Kumar K, Kumar K K and Pant G B 1994 Diurnal asymmetry of surface temperature trends over India; *Geophys. Res. Lett.* **21(8)** 677–680, https://doi.org/10.1029/94GL00007.

Salas J D 1993 Analysis and modeling of hydrologic time series. In: *Handbook of hydrology* (ed.) Maidment D R, McGraw-Hill, New York, pp. 19.1–19.72.

Santer B D, Wigley T M L and Taylor K E 2011 The reproducibility of observational estimates of surface and atmospheric temperature change; *Sci.* **334(6060)** 1232–1233, https://doi.org/10.1126/science.1216273.

Semenov M A and Porter J R 1995 Climatic variability and the modelling of crop yields; *Agric. Forest. Meteorol.* **73(3–4)** 265–283, https://doi.org/10.1016/0168-1923(94)05078-K.

Sen P K 1968 Estimates of the regression coefficient based on Kendall's tau; *J. Am. Stat. Assoc.* **63(324)** 1379–1389, https://doi.org/10.1080/01621459.1968.10480934.

Sharma U C 2003 Impact of population growth and climate change on the quantity and quality of water resources in the northeast of India; *IAHS Publ.* **281** 349–357, https://api.semanticscholar.org/CorpusID:132181883.

Singh D, Ghosh S, Roxy M K and McDermid S 2019 Indian summer monsoon: Extreme events, historical changes, and role of anthropogenic forcings; *Wiley Interdiscip. Rev.: Clim. Change* **10(2)** e571, https://doi.org/10.1002/wcc.571.

Smith L C 2000 Trends in Russian Arctic river-ice formation and breakup, 1917 to 1994; *Phys. Geogr.* **21(1)** 46–56.

Srivastava H N, Dewan B N, Dikshit S K, Rao G P, Singh S S and Rao K R 1992 Decadal trends in climate over India; *Mausam* **43(1)** 7–20, https://doi.org/10.54302/mausam.v43i1.3312.

Stocker T F, Qin D, Plattner G K, Alexander L V, Allen S K, Bindoff N L and Xie S P 2013 Technical summary; In: *Climate change 2013: The physical science basis,* Contribution of Working Group I to the Fifth Assessment Report of the Intergovernmental Panel on Climate Change, Cambridge University Press, pp. 33–115.

Tabari H, Abghari H and Hosseinzadeh Talaee P 2012 Temporal trends and spatial characteristics of drought and rainfall in arid and semiarid regions of Iran; *Hydrol. Process.* **26(22)** 3351–3361, https://doi.org/10.1002/hyp.8460.

Tabari H, Marofi S, Aeini A, Talaee P H and Mohammadi K 2011 Trend analysis of reference evapotranspiration in the western half of Iran; *Agric. Forest. Meteorol.* **151(2)** 128–136, https://doi.org/10.1016/j.agrformet.2010.09.009.

Vinnikov K Y, Groisman P Y and Lugina K M 1990 Empirical data on contemporary global climate changes (temperature and precipitation); *J. Clim.* **3(6)** 662–677, https://doi.org/10.1175/1520-0442(1990)003%3C0662:EDOCGC%3E2.0.CO;2.

Yue S and Hashino M 2003 Temperature trends in Japan: 1900–1990; *Theor. Appl. Climatol.* **75** 15–27, https://doi.org/10.1007/s00704-002-0717-11.

Yunling H and Yiping Z 2005 Climate change from 1960 to 2000 in the Lancang River Valley; *China Mt. Res. Dev.* **25(4)** 341–348, https://doi.org/10.2307/3674441.

Corresponding editor: PARATHASARATHI MUKHOPADHYAY